

Thermal and Dynamic Mechanical Characterization of Acrylic Bone Cements Modified with Biodegradable Polymers

E. Franco-Marquès,¹ J. A. Méndez,¹ J. Gironès,² M. A. Pèlach¹

¹LEPAMAP Group, University of Girona, EPS, Campus Montilivi, 17071 Girona, Spain

²Department of Polymeric Nanomaterials and Biomaterials, Institute of Polymer Science and Technology, CSIC, Madrid, Spain

Correspondence to: J. A. Méndez (E-mail: jalberto.mendez@udg.edu)

ABSTRACT: In this work, a thermal and a dynamic mechanical study of new formulations self-curing acrylic bone cements is reported. The basic formulation of poly(methylmethacrylate) (PMMA)-based acrylic bone cements has been modified with biodegradable polyesters such as poly(L-lactic acid), poly(β -hydroxybutyrate), and different kinds of thermoplastic starches. Differential scanning calorimetry (DSC) (dynamic and isothermal conditions), thermogravimetric analysis (TGA), dynamic mechanical thermal analysis (DMTA), and scanning electron microscopy (SEM) were used to determine the influence of the biodegradable polymer in the behavior of the biomedical formulations. DSC assay revealed a strong dependence of the polymerization enthalpy (ΔH_{cur}) with increasing solid : liquid ratio and a low influence of the nature of the added biodegradable polymer on glass transition. TGA analysis showed the different mechanism of PMMA-biodegradable polymer interaction depending on the solubilization of the added polymer in methylmethacrylate monomer during curing. DMTA showed the reinforcing capacity of segregated phases of the polymer included in the cement. The solubilization of aliphatic polyesters in the resulting PMMA polymerized phase led to a drop in mechanical stiffness observed from storage modulus (E') profiles. Moreover, $\tan \delta$ shifts to higher temperatures (4–7°C) during a second scan, confirming the presence of residual monomer content. © 2012 Wiley Periodicals, Inc. *J. Appl. Polym. Sci.* 000: 000–000, 2012

KEYWORDS: biomaterials; glass transition; differential scanning calorimetry (DSC); thermogravimetric analysis (TGA)

Received 21 June 2011; accepted 28 August 2012; published online

DOI: 10.1002/app.38523

INTRODUCTION

Acrylic cementation is a surgical technique often used for fixation of prosthesis, such as hip or knee, vertebra fracture reduction, bone defect filling and, in some cases, a methodology for bone tumor treatment.¹ This technique is based on the utilization of an “*in situ*” self-curing material to fix the prosthesis to the bone cavity and/or repair bone defects.

The basic formulation of acrylic bone cements is obtained by mixing a poly(methylmethacrylate) (PMMA)-based micro-sized powder (solid phase) with the methylmethacrylate monomer (MMA) (liquid). The curing process of MMA is initiated by a red-ox initiator system delivering free radicals to start the “*in situ*” polymerization and the subsequent hardening of the material during surgery. The result is a connective material, with no adhesive capacity, that transfers stresses from the body to the prosthesis or even treats tumor cells by a hyperthermia mechanism.¹

Physicochemical and biological properties of formulations of acrylic bone cements have been improved through modifying

the composition of both solid and liquid phases. In this sense, the addition of an opacifier is one of most often studied. For many years, barium sulfate has been incorporated to the solid phase to promote radiological control of the implant after surgery. More recently, novel synthetic opacifiers carrying halides have been tested to avoid incorporation of these inorganic salts.^{2–7} Thus, systems such as 3,5-diiodine salicylic methacrylate, 2,5-diiodo-8-quinolyl methacrylate, or other diiodine benzoyl derivatives have been effectively synthesized and copolymerized during curing with the monomer to allow radiological monitoring of the implant.

Traditionally, volumetric shrinkage during curing has been another limitation in the preparation of acrylic bone cements. Different approaches, using di-functionalized methacrylates such as 2,2-bis [4(2-hydroxy-3-methacryloxypropoxy) phenyl] propane (Bis-GMA),⁸ ethylene, or triethylenglycol dimethacrylate,⁹ have led to a decrease in the volumetric shrinkage as well as a significant improvement in mechanical properties.^{10,11} From the point of view of the red-ox initiator system, the use of tertiary amines (such as 4 -N, N-dimethylaminobenzoyl laurate,¹² 4,4-

dimethylamino benzoyl alcohol,¹³ or 4,4'-(dimethylamino)diphenyl carbinol (BZN)^{14,15} has demonstrated to induce lower toxicity than the commonly used *N*, *N*-dimethylamino-4-toluidine.

Nevertheless, the modification of none of these components enhances the integration of the implant with the newborn tissue, making biocompatibility and long-term stability difficult. In this sense, the incorporation of biodegradable constituents to the formulation opens new areas of knowledge to induce interaction capacity and promote cell growing. The incorporation of biodegradable polymers such as poly(ϵ -caprolactone),^{16,17} polysaccharides,^{18,19} or even bioceramics^{20,21} offers new possibilities of tissue-material interaction. It has been proved that, under some conditions, the biodegradation/solubilization process of these components may lead to tissue conduction and/or drug delivery through micropores formation. On the other side, the incorporation of inorganic bioactive or phosphate glasses improved the mechanical properties of the bone cements and enhanced bone integration through the generation of a layer of hydroxyapatite on the surface of the implant.

Most of the aforementioned modifications are based on laboratory synthesized materials or compounds, which increase the price of the formulations making difficult their up scaling to commercial exploitation. For this reason, our research has been focused toward inducing benefits to acrylic bone cements by using already commercialized polymer matrices. In a previous work, a preliminary study on the modification of a conventional acrylic bone cement and its possible application as drug delivery system of bisphosphonates has been reported.²² The modification was based on the addition of different commercial biodegradable polyesters and thermoplastic starches aiming for the development of formulation as drug delivery vehicle. In this work, an extended thermal and dynamic mechanical characterization of these modified formulations of acrylic bone cements has been carried out in order to improve understanding of the modification of the cements. Energetic parameters related with the curing process, such as enthalpy of polymerization (ΔH_{cur}), have been determined. In addition, the temperature of maximum decomposition rate ($T_{\text{d, max}}$) and the glass transition temperature (T_{g}) of the formulation prepared have also been determined and used to evaluate the effect of the solubility of the biodegradable polymers in the monomer during curing. Finally, the reinforcing capacity of the biodegradable microparticles has also been evaluated by dynamic mechanical thermal analysis (DMTA).

MATERIALS AND METHODS

Materials

PMMA microspheres (DegacrylTM MW 332) were provided by Degussa with an average diameter in the range of 40–45 μm . MMA was obtained from Acros Organics and used without any prior purification. Benzoyl peroxide, obtained from Scharlau and purified by fractional recrystallization from methanol (m_p 104°C), and BZN (Fluka) were used as low-temperature red-ox initiator system. PMMA microspheres were partially substituted by different biodegradable polymers namely: poly(L-lactic acid) (PLLA) (L9000, Biomer), poly(β -hydroxybutyrate) (PHB) (P226, Biomer),

aliphatic polyester (APP) with a melting temperature of 74°C (Mater-Bi TF01U/095 R, Novamont), thermoplastic starch (TPS1) (Mater-Bi YI014U/C, Novamont), and thermoplastic starch (TPS2) (Biopar, Avebe). All polymers were supplied in the shape of pellets.

Methods

Milling of Biodegradable Polymers. To improve the dispersion of the polymers within the bone cement, the pellets of the biodegradable polymers were milled to a size close to that of PMMA microspheres. Milling was carried out in an electrical mill, equipped with a set of stainless steel blades. After milling, particles were fractionated by means of sieves with 300 μm , 150 μm , and 75- μm mesh size.

Formulation of Partial Biodegradable Self-Curing Systems. The content of biodegradable polymer for each formulation was fixed at 33 wt %. To obtain low viscous and easy handling formulations, the solid : liquid ratio (*S* : *L*) was adjusted depending on two parameters: nature of the biodegradable polymer and its particle size. Formulations have been designated as follows: *X*-*Y*-*Z*, where *X* is added polymer, *Y* is its maximum particle size, and *Z* is the solid : liquid ratio (*S* : *L*). For example, the formulation “PLLA-300-1” was modified with PLLA, with a particle size between 300 and 150 μm , using a solid : liquid ratio of 1 : 1. PMMA reference formulations have been named as PMMA-*Z*, being *Z* the solid : liquid ratio (*S* : *L*).

Polymerization of Self-Curing Polymer Systems. As previously stated, the solid phase of the partially biodegradable self-curing formulations was prepared including different amounts of biodegradable polymer, depending on the solid : liquid ratio. Liquid phase was composed by the monomer (MMA) and BZN (1.0 wt %). Polymerization started with the addition of the liquid phase to the solid one. Initially, the reacting mass was hand-stirred with a spatula at a very low mixing rate (20–30 rpm) to avoid immobilized air bubbles. Once the reacting mass did not stuck to the surgical glove, it was molded. Finally, the mold was placed in an electric oven at 37°C for 1 h, to simulate physiological conditions.

Surface Characterization (SEM). The particles of the biodegradable polymers and the surface of the modified acrylic bone cements were characterized by scanning electron microscopy (SEM). Fractured surfaces of molded specimens, frozen under liquid nitrogen, were sputter-coated with gold (K550 from Emitech, Ashfort, UK) and observed under a Zeiss DMS 960 model electronic microscope.

Curing Process Monitoring (Isothermal-DSC). A mass of 5 g of each acrylic bone cement formulation was prepared following standard procedure mentioned above. Later on, a small aliquot of 15–20 mg of this reacting dough was quickly transferred to an aluminum pan and placed in a differential scanning calorimeter (DSC 822^e, (Mettler-Toledo (Switzerland); accuracy: 0.2°C, reproducibility: 0.1°C), under nitrogen atmosphere (40 mLmin⁻¹), at 25°C. Exothermic process was recorded and the evolved energy [ΔH_{cur}] was calculated from the area under the curve heat flow versus curing time. This experiment was driven per duplicate to confirm the values of temperature and ΔH_{cur} .

Thermal Resistance Evaluation (TGA). Thermogravimetric analysis (TGA) was carried out in a TGA/DTA 851^e Mettler-

Toledo thermal analyzer (Switzerland). Samples (8–10 mg) of cured samples were heated from 50 to 600°C at a heating rate of 10°C min⁻¹ under nitrogen atmosphere (40 mLmin⁻¹). The thermograms were converted to derivative weight percent to determine the temperature of maximum decomposition rate ($T_{d, \max}$). This experiment was driven per duplicate to confirm the profiles of degradation.

Thermal Transitions Determination (Dynamic-DSC). Glass transition temperature (T_g) was determined by DSC using a DSC-30 calorimeter (Mettler-Toledo, Switzerland). Samples (15–20 mg) of each material were heated from 50 to 150°C at a heating rate of 10°C min⁻¹ under nitrogen atmosphere (40 mLmin⁻¹). Two scans were performed: (1) removal of thermal history; (2) after cooling to start temperature, the samples were heated again at the same heating rate to 150°C. This experiment was driven per duplicate to confirm the values of temperature.

Dynamic Mechanical Thermal Evaluation. Dynamic mechanical thermal analysis (DMTA) of the self-cured formulations was performed, from room temperature to 140°C at a heating rate of 3°C min⁻¹ under nitrogen atmosphere (80 mLmin⁻¹), in a DMA/SDTA 861 ° (Mettler-Toledo (Switzerland)) analyzer. The analyses were performed on a dual cantilever setup with a controlled displacement of $\pm 30 \mu\text{m}$ (about $\pm 1 \text{ N}$ in force). The dimensions of the samples were cut to $13 \times 3 \times 42 \text{ mm}^3$. Two scans were performed. Once the first scan was performed, the sample was cooled to room temperature and subsequently heated again to 140°C at the same heating rate. This experiment was driven per duplicate to confirm the profiles of E' with temperature.

RESULTS AND DISCUSSION

In this work, a complementary physicochemical study, based on thermal and dynamic mechanic thermal characterization has been carried out to improve the understanding of a biomedical characterization previously reported.²² This study supplies important information about processing, component interactions, heat damage risk, and even the presence of undesired components that is too often overlooked/ignored.

Morphology

The milling of the biodegradable polymer pellets, under liquid nitrogen, produced microparticles with nonhomogeneous particle surface. Any thermal history is expected to be induced in the powder due to all the milling process was carried out in a very short period of time and keeping the sample at a very low temperature. The use of a milling system based on blades led to microparticles with random edges as shown in Figure 1(SEM images A–C). This result was shared by all milled materials prepared in this work. Nevertheless, this irregular surface morphology is not an impediment for the incorporation of the milled polymer into the cement. As showed in Figure 1(SEM image D), particles were homogeneously distributed inside the PMMA matrix of the acrylic bone cement. Neither aggregates nor unbounded interfaces could be observed between PMMA and TPS1, even when large size particles were used, contributing to mechanical enhancement. The literature reports that the transfer of stresses from PMMA to the reinforcing agent, even the stiff-

ness of the composite, are improved with increasing particle individualization in the final composite.^{23,24}

Curing Process

Dough time (mixing time) should be lower than 5 min according to ISO 5833. The mixing time of the formulations synthesized in this work was in the range of 2–6 min depending on solid : liquid ratio being shorter when larger solid : liquid ratios are used. Mixing time increases with decreasing solid : liquid ratios due to a larger amount of monomer delays the vitrification process of the system. ISO 5833 standard also specifies the procedure for determining the curing parameters of acrylic bone cements. By following this procedure, the results of maximum temperature achieved during curing are determined without obtaining information regarding the delivered energy. However, because the exothermic energy and its link with the solid : liquid ratio of the formulation are the responsible of thermal toxicity (necrotic processes) of the surrounding tissue, its determination has been taken into account. Figure 2(A) shows the heat flow versus curing time profile of the curing process of the plain-PMMA acrylic bone cement formulations. An exothermic process attributed to the polymerization of MMA of the liquid phase was observed and the value of its polymerization enthalpy (ΔH_{cur}) was measured from the area under the exothermic peak. Table I summarizes ΔH_{cur} of the curing process and the $t_{\text{onset}}/t_{\text{max}}/t_{\text{endset}}$ times for each thermogram.

PMMA-2, PMMA-1.5, and PMMA-1 have been tested as reference materials to give a broad overview of the formulations prepared in this work. Their curing profiles are showed in Figure 2(B). The incorporation of higher content of MMA in the formulations, as evidenced when solid : liquid ratio was decreased from 2 to 1, led to higher values of ΔH_{cur} . This result is consistent with the presence of higher amounts of MMA during the curing process. The higher is the monomer content, the higher is the energy delivered. Moreover, ΔH_{cur} were in the range of 107–270 J g⁻¹, depending on monomer content, very far from the enthalpy of polymerization of methyl methacrylate (ΔH_p) (577 J g⁻¹, Ref. 25). This low delivery of energy can be explained by the presence of the PMMA microspheres during curing. PMMA has a low thermal conductivity (0.19 W m⁻¹ K⁻¹),²⁶ obstructing the transmission of energy from the bulk to the external medium. This behavior has previously been reported for cements modified with inorganic glasses to induce bioactive character.²⁷ In that work, the presence of the inorganic particles reduced peak temperature by 10–20°C.

ΔH_{cur} also decreased after the incorporation of commercial biodegradable polymers to the cement formulation. Again, the decrease in the exothermic energy was higher for the formulations with higher solid : liquid ratio ($S : L$). This result can also be attributed to the fact that, in this work, the formulations with higher $S : L$ ratio were prepared with polymer particles with higher size. It is expected that the use of particles with higher size (300 μm) also could cause a decrease in the heat transfer, leading to a lower delivery of energy to the body. Moreover, in the clinical practice, the effect of the exothermic heat is lower because the material is applied in a thin layer, there is some contact with blood circulation and the heat is

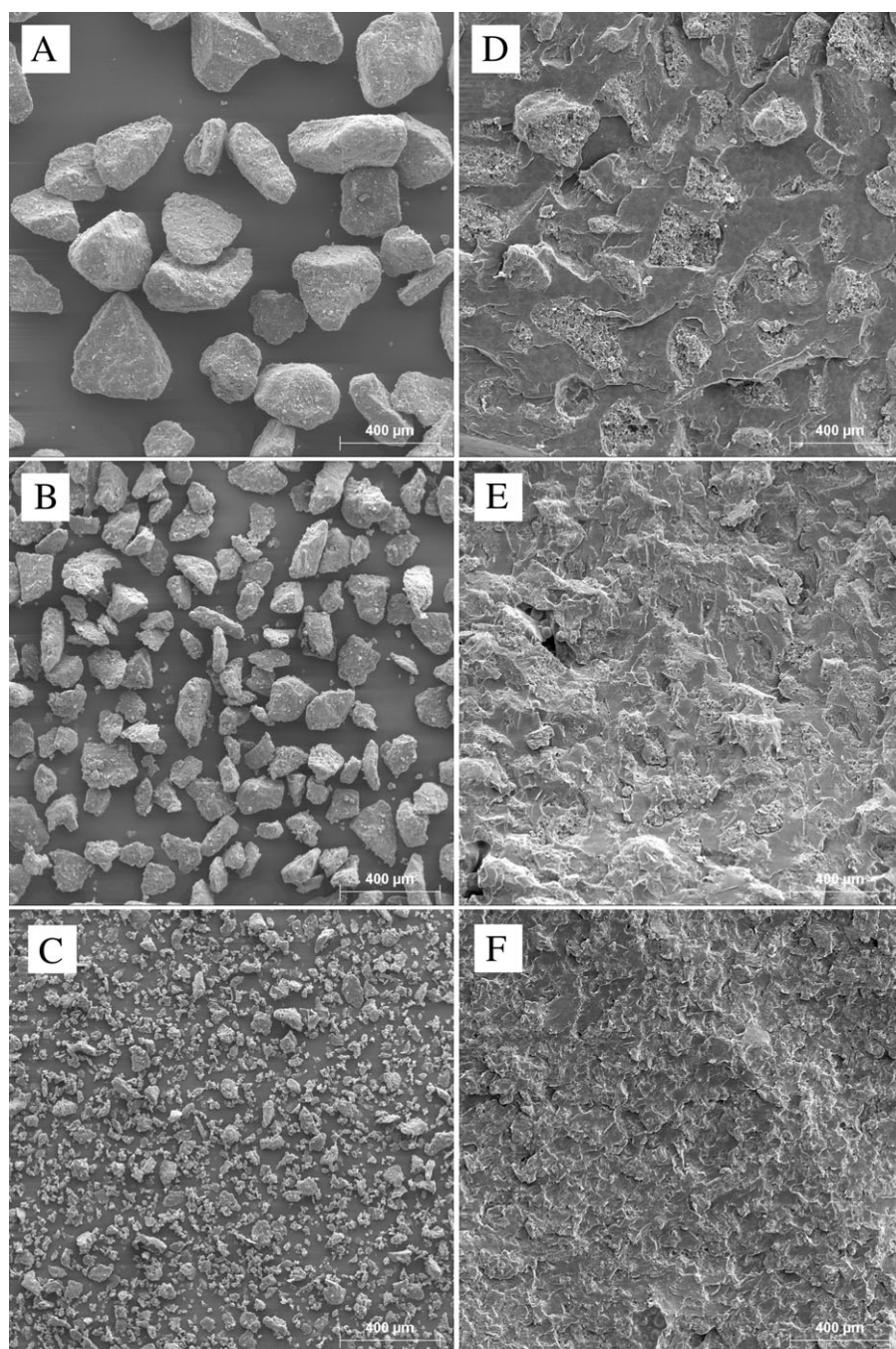


Figure 1. SEM micrographs of TPS1-based particles (left) and surfaces of derived acrylic bone cements (right). Up: 300 μm , middle: 150 μm , down: 75 μm .

dissipated due to the contact between the cement and the prosthesis.²⁸ This effect is very favorable because it minimizes the risk of necrosis in the surrounding tissues. A decrease in the peak temperature can also be expected, as demonstrated in the previous work, for the same self-curing formulations.²² Moreover, this lower peak temperature also is expected to be responsible of the presence of residual monomer content and consistently with a lower curing level. Lower polymerization temperature involves higher viscosity and lower diffusion capacity of the monomer through the polymerizing mass.²⁹

Thus, a lower curing temperature of the formulations modified with biodegradable polymers, regarding PMMA control, leads to higher monomer content as previously reported. This hypothesis is consistent with the increase of T_g of the system after a second scan in DMTA that will be discussed later.

The term t_{onset} represents the start of the exothermic peak. Taking into account the PMMA references, t_{onset} is longer for formulations with lower $s : l$ ratio. This effect can be assigned to the delay in viscosity increase (and consequently in the

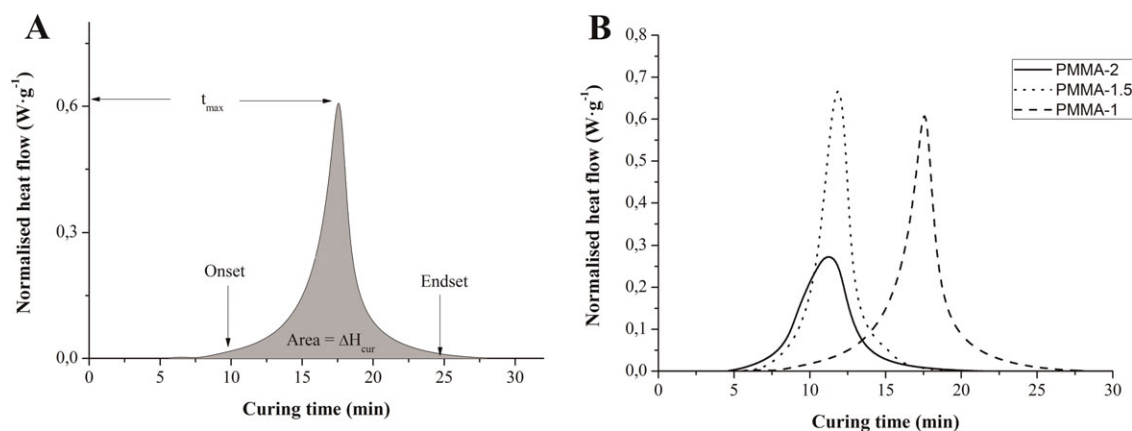


Figure 2. Isothermal-DSC thermograms. Heat flow versus curing time of (A) PMMA-2 and (B) comparative of plain PMMA references.

termination stage of the polymerization) with increasing monomer content. The formulations modified with APPs showed a longer t_{onset} when compared with their corresponding PMMA references. The reason may lay in the fact that the presence of polyester particles restricts the diffusion of the monomer through the curing mass, delaying the polymerization process. PLLA-300-1 also showed a longer value of t_{onset} compared with the other two formulations modified with APPs, due to the use of a lower $s : l$ ratio. In the case of the materials modified with TPS1 and TPS2, the formulation with the smallest particles had larger t_{onset} values, again attributed to the lower $s : l$ ratio.

From the point of view of the time to reach maximum heat emission (t_{max}), a decrease has been observed in the formulations modified with biodegradable polyesters and polysaccharides. Moreover, the width of the peak is also narrower than that of corresponding plain PMMA reference, as reported in Table I. This phenomenon is also very interesting because it helps to minimize necrotic and inflammatory effects to surrounding tissues because the curing process spends less time at high temperature.

Thermal Stability

Thermal stability has been evaluated by TGA. Obviously, the thermal resistance of these materials is expected to be much higher than that required for their suggested application. Nevertheless, its study can give an important information regarding the structure-properties of the material. Figure 3 shows the degradation profiles of the materials analyzed, whereas Table II summarizes their characteristic temperatures, obtained from the first TGA derivative. The degradation profile of the formulation APP-300-2, modified with Mater-Bi TF01U/095 R APP, is showed in Figure 3(A). The incorporation of APP powder increased the temperature of maximum decomposition rate ($T_{d, \text{max}}$) more than 55°C (compared with plain PMMA formulation used as reference) displaying a single decomposition process. In the case of the formulations modified with PHB and PLLA, a different behavior has been observed. The PHB-modified formulation showed a thermal decomposition in two steps, each of them located close to the degradation of its individual homopolymeric components (PHB and PMMA), as observed in Figure 3(B). As for the PLLA-300-1 formulation, it displayed a single thermal decomposition [Figure 3(C)] with a maximum rate of

decomposition close to PLLA and PMMA values. The different behavior of these three formulations can be explained by means of two parameters: (1) partial solubilization of the biodegradable polymer in the monomer during curing, and (2) the individual $T_{d, \text{max}}$ of the components of the cement. In the case of the APP-300-2 formulation, it must be taken into account that the APP polyester is soluble in methylmethacrylate at temperatures above $35\text{--}40^{\circ}\text{C}$. Thus, because the curing process of this system reaches temperatures close to 50°C ,²² partial solubilization of APP in MMA monomer occurs during processing. Solubilization leads to better dispersed APP-PMMA blends, avoiding the presence of big domains of pure APP in the cement and giving rise to a single degradation process at temperatures between those of the two polymers. To confirm this hypothesis, the surface of APP-300-2 material was analyzed by SEM (Figure 4). In clear contrast with images showed in Figure 1 (corresponding to starch based formulations), individual particles of APP cannot be clearly observed on the surface of the material, corroborating that APP particles had been partially dissolved by the monomer during curing. Moreover, small holes are observed

Table I. Curing Enthalpy and Characteristic Times in the Curing Process of Acrylic Bone Cements Modified with Biodegradable Polyesters and Polysaccharides

Formulation	ΔH_{cur} (J g ⁻¹)	t_{onset} (min)	t_{max} (min)	t_{endset} (min)	Δt (min)
PMMA-2	69.3	4.7	11.2	18.7	14.0
PMMA-1.5	108.1	6.4	11.9	17.4	11.0
PMMA-1	117.0	10.3	17.6	24.8	14.5
APP-300.2	72.0	5.5	10.5	15.5	10.0
PHB-300-2	59.3	5.0	12.2	18.1	13.1
PLLA-300-1	154.5	9.2	15.7	22.0	12.8
TPS1-300-2	59.2	6.3	10.5	13.4	7.1
TPS1-150-1.5	72.6	5.2	9.8	15.4	10.2
TPS1-75-1	117.0	8.6	14.3	19.3	10.7
TPS2-300-2	56.2	5.2	9.5	15.4	10.2
TPS2-150-1.5	72.6	5.2	9.8	15.4	10.2
TPS2-75-1	117.2	8.6	14.3	19.3	10.7

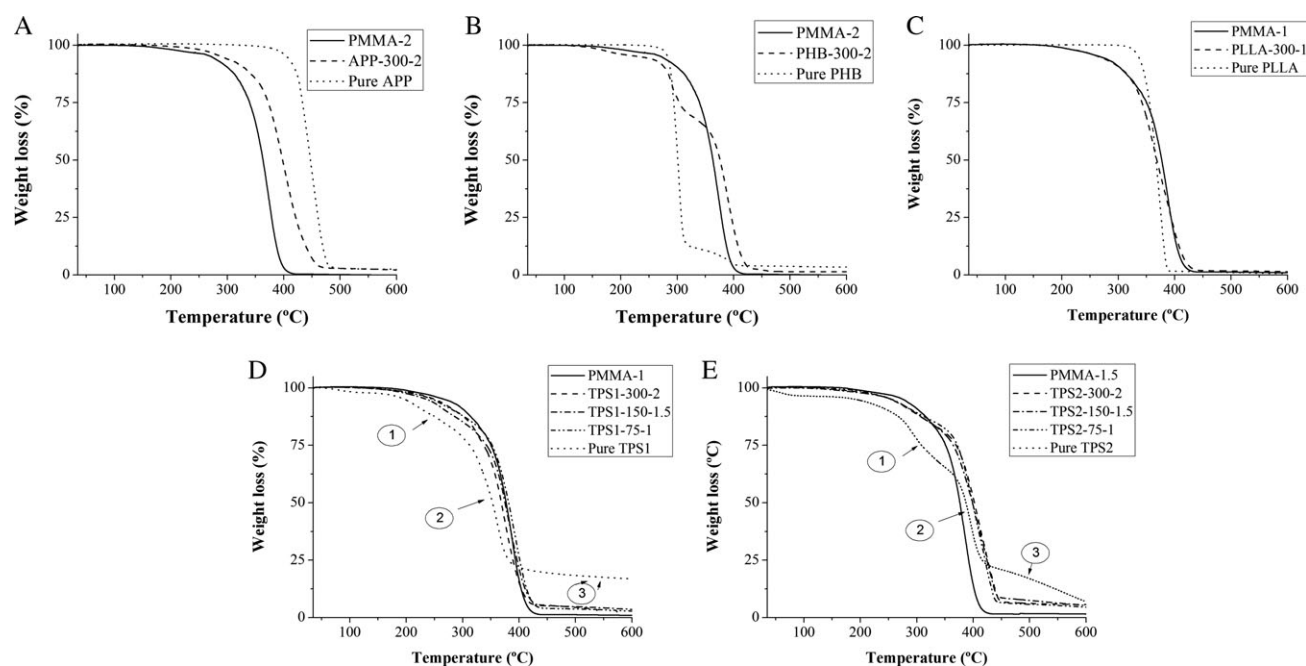


Figure 3. TGA thermograms: (A) APP-300-2, (B) PHB-300-2, (C) PLLA-300-1, (D) cements modified with TPS1, and (E) cements modified with TPS2. Mrd: maximum rate of decomposition.

due to the presence of air bubbles trapped during mixing handmade process. In the case of the formulation PHB-300-2, its peak temperature during curing had been previously reported to be close to 60°C.²² Because there is not solubilization of PHB in MMA phase even at 80°C, a system with dispersed particles of PHB in the polymerized PMMA phase was obtained (as can be observed in Figure 5). Because of $T_{d, \max}$ of PHB being very different to that of PMMA (300°C and 373°C, respectively), two well-defined degradation stages can be observed on TGA curves. The behavior of the formulation of PLLA-300-1 is analogous to PHB-300-2 and no solubilization of the biodegradable polymer in the monomer occurs. However, $T_{d, \max}$ of PLLA and PMMA are quite close, and as a consequence, a single degradation stage is observed.

Finally, the materials modified with the different commercial thermoplastic starches, Mater-Bi YI014U/C (TPS1) and Biopar (TPS2), showed a similar behavior [Figure 3(D, E), respectively]. In both cases, a small loss of weight can be observed at temperatures close to 100°C, attributed to the evaporation of absorbed water. Thermal degradation of plain thermoplastic starches takes place in three steps.³⁰ The first stage (230–280°C) is related with the evaporation of low molecular weight plasticizers such as glycerol; the second stage (320–350°C) is basically related with the thermal decomposition of the native polysaccharide; the third stage corresponds to the degradation of the polymer added to native starch to promote thermoplasticity, being (poly(ethylene-co-vinyl alcohol) the often used.^{31,32} Anyhow, in both cases [Figure 3(D, E)], $T_{d, \max}$ is not damaged by the incorporation of the biodegradable component (compared with that of PMMA-1). By the opposite, this addition led to values of $T_{d, \max}$ even slightly higher than that of PMMA, corroborating the existence of microdomains of the thermoplastic starch in the cement. Concerning

the effect of particle size, it was observed that the size of starch powders did not affect to the thermal degradation of the material.

Glass Transition Temperature (T_g)

The evaluation of glass transition temperature (T_g) can offer information not only about the processability of amorphous materials but also about curing yield and other energetic aspects of the transition.³³

Table II. Onset Temperature and Temperature of Maximum Rate of Degradation (T_{mrd}) of Acrylic Bone Cements

Formulation	First degradation step		Second degradation step	
	T_{onset} (°C)	$T_{d, \max}$ (°C)	T_{onset}^* (°C)	$T_{d, \max}^*$ (°C)
PMMA-2	318	373		
PMMA-1.5	335	386		
PMMA-1	339	388		
APP-300-2	336	400		
PHB-300-2	261	291	345	389
PLLA-300-1	297	380		
TPS1-300-2	234		320	374
TPS1-150-1.5	219	265	334	383
TPS1-75-1	241		328	394
TPS2-300-2	227	286	345	410
TPS2-150-1.5	237	292	339	421
TPS2-75-1	240	284	347	422

*, Temperature of a second degradation step (if exist).

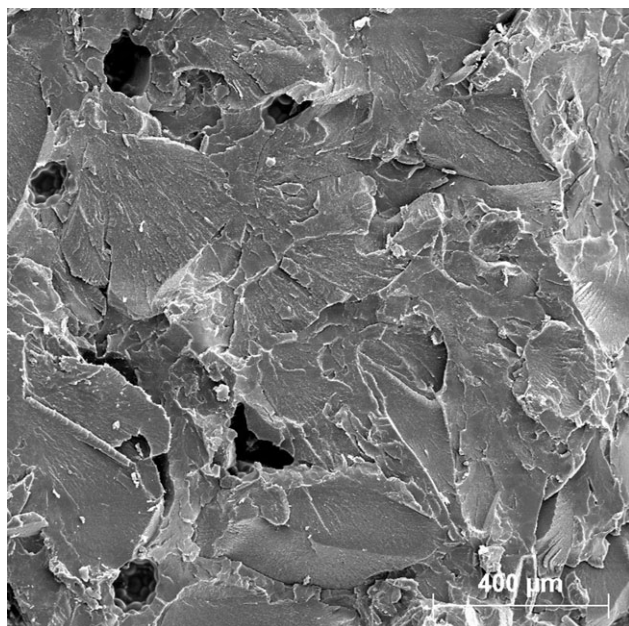


Figure 4. SEM micrograph of the surface of APP-300-2.

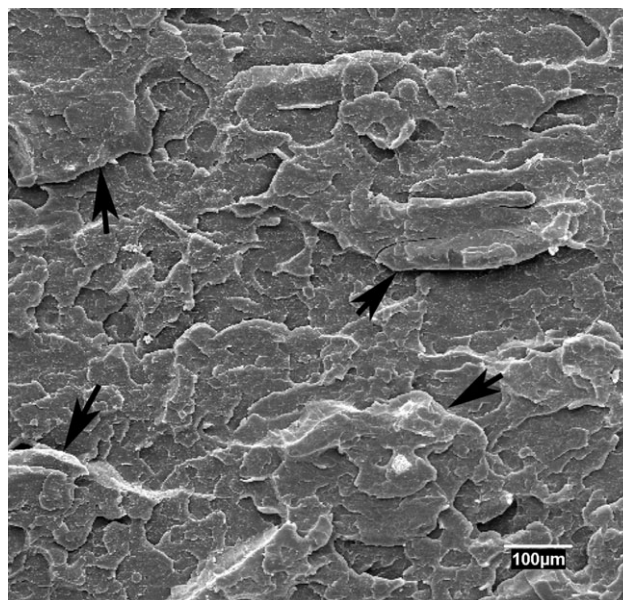


Figure 5. SEM micrograph of the surface of PHB-300-2. Black arrows identify nonsoluble particles of PHB inside PMMA matrix.

Table III and Figure 6 summarize the results of the DSC characterization of the materials prepared. PMMA beads used in this work presented a glass transition around 115°C. Once PMMA reference materials were cured, glass transition decreased approximately by 8–9°C, independently on the solid : liquid ratio used. Moreover, the interval of the transition was slightly enlarged from 13.8 min to 15.7 min. Both phenomena are related with the polymerization of MMA and the presence of PMMA beads. The decrease in T_g after curing can be related with the presence of residual monomer content. According to Craig,³⁴ lower T_g is caused by an incomplete polymerization of

the monomer. Because of the low molecular weight of MMA, compared with PMMA, this monomer affects both biological and physical viability of the material. From the point of view of biological acceptance, MMA can be leached from the implanted material to blood. This behavior may evolve into cardiorespiratory and vascular dysfunctions during hip prosthesis surgery, being a possible driver of blood flow disturbance and hemolytic processes.^{35,36} In the case of the physical influence, the presence of monomeric MMA, as a low molecular weight molecule, induces a plasticizing behavior that causes a drop in mechanical properties, a hypothesis further corroborated by DMTA

Table III. Glass Transition Temperature (T_g) of Acrylic Bone Cements Measured by Means of DSC (Dynamic Mode) and DMTA

Formulation	DSC				DMTA	
	T_g^{DSC} (°C)	T_g^{DSC} Onset (°C)	T_g^{DSC} Endset (°C)	ΔT_g^{DSC} (°C)	T_g^{DMTA} (°C)*	T_g^{DMTA} (°C)**
PMMA (beads)	115.6	108.7	122.5	13.8	–	–
PMMA-2	106.5	98.6	114.3	15.7	122.5	125.8
PMMA-1.5	106.2	96.9	115.5	18.6	123.8	126.2
PMMA-1	107.0	97.7	116.2	18.5	124.8	128.7
APP-300-2	–	–	–	–	118.2	123.8
PHB-300-2	–	–	–	–	110.1	114.7
PLLA-300-1	–	–	–	–	112.1	116.6
TPS1-300-2	–	–	–	–	116.0	116.7
TPS1-150-1.5	–	–	–	–	115.5	117.0
TPS1-75-1	100.4	87.5	107.3	19.8	114.1	118.6
TPS2-300-2	105.3	95.4	115.3	19.9	120.4	123.4
TPS2-150-1.5	106.1	97.5	114.6	17.1	118.0	124
TPS2-75-1	106.8	95.3	118.4	23.1	117.4	125.79

*, First scan; **, Second scan.

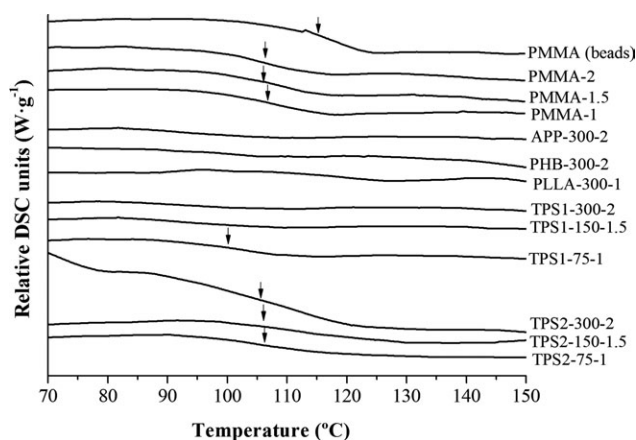


Figure 6. Dynamic-DSC thermograms of acrylic bone cements modified with biodegradable polyesters and thermoplastic starches.

experiments detailed below. On the other side, the different molecular weight and polydispersity of commercial PMMA beads and the newly polymerized MMA phase must be taken into consideration, particularly considering their different polymerization conditions: suspension, for the PMMA beads, and bulk polymerization, for new “*in situ*” polymerized phase. Suspension and bulk polymerization are polymerization systems with different behavior of monomer diffusion.²⁹ This different behavior

leads to different propagation and termination stages in the polymerization reaction. This phenomenon leads to values of molecular weight distribution slightly different, increasing the polydispersity of the system when both materials are mixed. The increase in the polydispersity resulted in a broader interval of glass transition and a shift on its temperature.

In the case of the materials modified with biodegradable polymers, there were some difficulties to determine glass transition because of the very low energy associated with this process. Change of heat flow during glass transition of the formulations had values around 0.1 W g^{-1} , too low to be well resolved by DSC. For this reason, glass transition temperatures have also been determined by means of dynamic mechanical thermal analysis (DMTA). T_g values have been read from the local maximum of $\tan \delta$ profile. Figure 7 and Table III summarize the results of the characterization of glass transition by means of DMTA assays. The values of T_g determined by DMTA are slightly higher than those obtained by DSC. This shift is caused by the different processes related with the determination of T_g . In the case of DSC, the evaluation of T_g is carried out under static conditions. By the opposite, on DMTA assays, sample is subjected to an oscillatory deformation (strain) at a constant frequency (1 Hz) that modifies its response. Nevertheless, all formulations modified with biodegradable polyesters showed a slight decrease in T_g when compared with the plain PMMA reference. As mentioned earlier, this decrease, in the range of

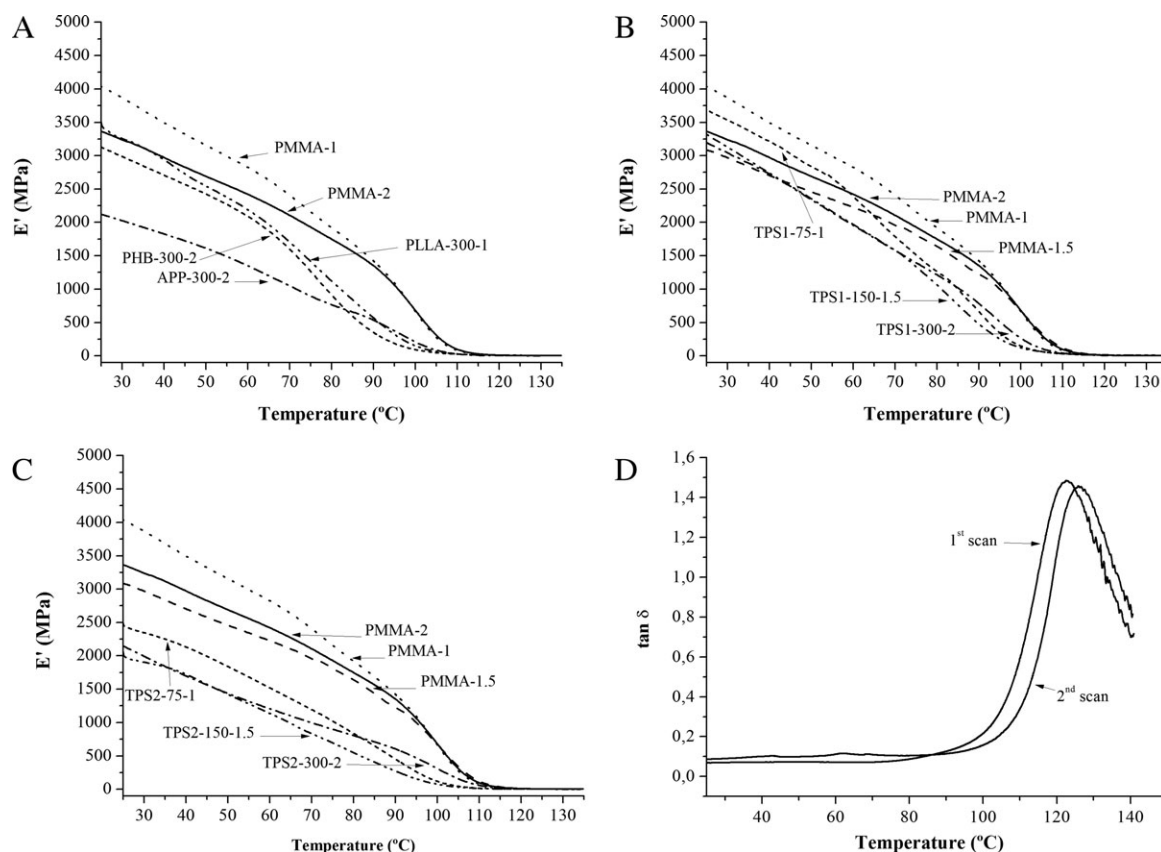


Figure 7. Storage modulus (E') profile of cements modified with (A) biodegradable polyesters, (B) TPS1, and (C) TPS2. (D) $\tan \delta$ profile of the first and second scan of PMMA-2.

7–12°C, can be assigned to the plasticizing effect of the non-reacted monomer. In fact, as previously reported,²² the incorporation of APP, PLLA, and PHB leads to higher values of residual monomer content (in the range of 2.16–4.03%), compared with that of the plain PMMA formulation (0.40%). Thermoplastic starches also induced a decrease in glass transition, although this phenomenon was mainly attributed to traces of water absorbed on the material due to its high hydrophilic character.

When second DMTA scan was performed, T_g shifted to higher values, compared with that of the first scan. This result points out to the occurrence of changes in the chemical structure of the material during first scan. A post curing of the residual monomer is assumed to happen at the end of the first scan, decreasing the content of low molecular weight species responsible of plasticizing phenomena. This result confirms the presence of residual monomer content previously observed in the previous work²² and justifies the low polymerization enthalpy of the cements mentioned above. The curing of the residue of monomer content is induced due to the energy given to the material during the heating of the first DMTA scan, what confirms that higher curing temperature leads to a lower monomer content as mentioned above. The presence of residual monomer content has also been reported in literature^{27,37} and its presence is the responsible of different toxic affections to cells and tissues.³⁸

Reinforcing Effect of Biodegradable Polymer Powders

Figure 7 shows the profiles of storage modulus (E') versus temperature of the bone cements modified with biodegradable polyesters and thermoplastic starches. As it can be observed, in all the cases evaluated, E' is lower than that of the reference of plain PMMA, evidencing the lower stiffness of these materials. APP-300-2 showed the lowest value of E' , in agreement with the partial solubilization of APP in the monomer during curing suggested. No reinforcing effect is observed, also in agreement with the absence of particles of pure APP in the material after curing. By the opposite, at 37°C, formulations modified with PLLA and PHB presented storage modulus of 3100 and 2750 MPa, respectively, which are between those of PMMA-1 (3600 MPa) and APP-300-2 (1800 MPa), representing a limited reinforcing capacity.

The cements modified with TPS1 and TPS2 also showed a decrease in E' , compared with references, particularly higher in the case on TPS1. This was an expected result considering the composition of this material. TPS1 is a commercial material designed for injection purposes, whereas TPS2 was designed for blowing, as mentioned in their corresponding datasheets. The different field of application of the two TPS correlates well with the mechanical properties of their respective composites.

Finally, the effect of particle size distributions was also evaluated. In the case of thermoplastic starches, the smallest particles (used for obtaining TPS1-75-1 and TPS2-75-1) had a better reinforcing effect than bigger ones. E' of TPS1-75-1, measured at 37°C, represents by 92% of the value of PMMA-1 formulation, what indicates the good reinforcing character of this material at low particle size. This interesting result is a consequence of the previously mentioned homogeneity and particle

integration observed by SEM on PMMA-TPS1 formulations. The better dispersibility of TPS particles in the cement leading to improved stiffness.

CONCLUSIONS

An intensive thermal and dynamic mechanical characterization of acrylic bone cements modified with commercial biodegradable polymers has been carried out. A previous manuscript described the potential use of these materials as drug delivery system in the treatment of osteoporosis. The present work helps to characterize the physicochemical aspects of the formulations to improve their understanding and application. Chemical structure (—OH functionalization, presence of residual monomer content, solid : liquid ratio, and the balance of compositions) and physical parameters (shape and size distribution of microparticles added to the cement, solubilization capacity of the biodegradable polymer in the reacting monomer, intrinsic mechanical properties of the added polymers) are critical parameters in the behavior of the cement. The exothermic character of the curing process is controlled by two main parameters: incorporation of microparticles to the curing material and the solid : liquid ratio. Added particles act as an energetic barrier against heat flow transmission and lower values of solid : liquid ratios lead to lower presence of nonreacted monomer after curing.

The solubilization of the added polymer in the monomer during curing represents an important drop in the stiffness of the material, observed from storage modulus of the material. On the contrary, the insoluble polymers in the monomer during curing, such as thermoplastic starch, allows obtaining moderate reinforced materials, representing an important advance in the preparation of economic formulation of acrylic bone cements, with a functional capacity (drug delivery), keeping their mechanical integrity.

ACKNOWLEDGMENTS

The authors thank to Ministry of Science and Innovation of Spain (MICINN) for financial support (project MAT2010-18155). E. Franco-Marquès thanks financial support to University of Girona, Spain (doctorate grant BR-07/05).

REFERENCES

1. Nelson, D. A.; Barker, M. E.; Hamlin, B. H. *Int. J. Hyperthermia* **1997**, *13*, 287.
2. Artola A.; Gurruchaga, M.; Vazquez, B.; San Roman, J.; Goñi, I. *Biomaterials* **2003**, *24*, 4071.
3. Davy, K. W. M.; Anseau, M. R.; Odlyha, M.; Foster, G. M. *Polym. Int.* **1997**, *43*, 143.
4. Ginebra, M. P.; Albuixech, L.; Fernandez-Barragan, E.; Aparicio, C.; Gil, F. J.; San Roman, J.; Vazquez, B.; Planell, J. A. *Biomaterials* **2002**, *23*, 1873.
5. Hernández, L.; Vázquez, B.; López-Bravo, A.; Parra, J.; Goñi, I.; Gurruchaga, M. *J. Biomed. Mater. Res. A* **2007**, *80A*, 321.
6. Hernandez, L.; Fernandez, M.; Collia, F.; Gurruchaga, M.; Goñi, I. *Biomaterials* **2006**, *27*, 100.

7. Kruft, M. A.; Benzina, A.; Blezer, R.; Koole, L. H. *Biomaterials* **1996**, 17, 1803.
8. Zhang, H.; Dravell, B. W. *J. Mech. Behav. Biomed. Mater.* **2012**, 10, 39.
9. Deb, S.; Vazquez, B.; Bonfield, W. *J. Biomed. Mater. Res.* **1997**, 37, 465.
10. Claudia, I.; Walter, F. S. *J. Biomed. Mater. Res. B* **2005**, 74B, 676.
11. Deb, S.; Aiyathurai, L.; Roether, J. A.; Luklinska, Z. B. *Biomaterials* **2005**, 26, 3713.
12. Vazquez, B.; San Roman, J.; Deb, S.; Bonfield, W. *J. Biomed. Mater. Res.* **1998**, 43, 131.
13. Méndez, J. A.; Vazquez, B.; Ginebra, M. P.; Gil, F. J.; Manero, J. M.; Planell, J. A.; San Román, J. *J. Appl. Biomater. Biomech.* **2003**, 1, 48.
14. de la Torre, B.; Fernández, M.; Vázquez, B.; Collía, F.; de Pedro, J. A.; López-Bravo, A.; San Román, J. *J. Biomed. Mater. Res. B* **2003**, 66B, 502.
15. de la Torre, B.; Salvado, M.; Corchón, M. A.; Vázquez, B.; Collía, F.; de Pedro, J. A.; San Román, J. *J. Mater. Sci.: Mater. Med.* **2007**, 18, 933.
16. Mendez, J. A.; Abraham, G. A.; Fernandez, M. D.; Vazquez, B.; San Roman, J. *J. Biomed. Mater. Res.* **2002**, 61, 66.
17. Abraham, G. A.; Vallo, C. I.; San Roman, J.; Cuadrado, T. R. *J. Biomed. Mater. Res. B* **2004**, 70B, 340.
18. Espigares, I.; Elvira, C.; Mano, J. F.; Vazquez, B.; San Roman, J.; Reis, R. L. *Biomaterials* **2002**, 23, 1883.
19. Mori, R.; Nakai, T. *Clin. Orthop. Relat. Res.* **2011**, 469, 600.
20. Mendez, J. A.; Vazquez, B.; Ginebra, M. P.; Gil, F. J.; Manero, J. M.; Planell, J. A.; San Roman, J. *J. Mater. Sci.: Mater. Med.* **2002**, 13, 1251.
21. Boesel, L. F.; Cachinho, S. C.; Fernandes, M. H.; Reis, R. L. *Acta Biomater.* **2007**, 3, 175.
22. Franco-Marques, E.; Mendez, J. A.; Girones, J.; Ginebra, M. P.; Pelach, M. A. *Acta Biomater.* **2009**, 5, 2953.
23. Cardoso, P.; Klosterman, D.; Covas, J. A.; van Hattum, F. W. J.; Lanceros-Mendez, S. *Polym. Test.* **2012**, 31, 697.
24. Park, J. M.; Wang, Z. J.; Kwon, D. J.; Gu, G. Y.; Lee, W. I.; Park, J. K.; Lawrence DeVries, K. *Compos. B* **2012**, 43, 2272.
25. Vazquez, B.; Gallardo, A.; Elvira, C.; San Román, J. In *Ciencia y Tecnología de Materiales Poliméricos, Volumen II*; Garrido, L.; Ibarra, L.; Marco, C., Eds.; Instituto de Ciencia y Tecnología de Polímeros, CSIC: Madrid, **2004**; Chapter 2.
26. Furuta, I.; Kimura, S. I.; Iwama, M. In *Polymer Handbook*, 4th ed.; Brandrup, J.; Immergut, E. H.; Grulke, E. A., Eds.; Wiley: New York, **1999**; Chapter V.
27. Mendez, J. A.; Fernandez, M.; Gonzalez-Corchon, A.; Salvado, M.; Collia, F.; de Pedro, J. A.; Levenfeld, B. L.; Lopez-Bravo, A.; Vazquez, B.; San Roman, J. *Biomaterials* **2004**, 25, 2381.
28. Kuehn, K. D.; Ege, W.; Gopp, U. *Orthop. Clin. North Am.* **2005**, 36, 17.
29. Odian, G. In *Principles of Polymerisation*, 3rd ed.; Odian, G., Ed.; Wiley: New York, **1991**; Chapter 3.
30. Vega, D.; Villar, M. A.; Failla, M. D.; Vallés, E. M. *Polym. Bull.* **1996**, 37, 229.
31. Matsuyama, H.; Kobayashi, K.; Maki, T.; Tearamoto, M.; Tsuruta, H. *J. Appl. Polym. Sci.* **2001**, 82, 2583.
32. Vega, D.; Villar, M. A.; Failla, M. D.; Vallés, E. M. *Polym. Bull.* **1996**, 37, 229.
33. Vallo, C. I.; Montemartini, P. E.; Cuadrado, T. R. *J. Appl. Polym. Sci.* **1998**, 69, 1367.
34. Hanks, C. T.; Kohn, D.; Koran, A., III; O'Brien, W. J.; Powers, J. M.; Wagner, W. C.; Wataha, J. C. *Restorative Dental Materials*, 10th ed.; Craig, R. G., Ed.; Harcourt Brace: St. Louis, **1997**.
35. Albrektsson, T.; Kinder, L. *Clin. Orthop. Relat. Res.* **1984**, 183, 280.
36. Cenni, E.; Ciapetti, G.; Granchi, D.; Savarino, L.; Stea, S.; Corradini, A. *Biomaterials* **2001**, 22, 1321.
37. Vallo, C. I.; Montemartini, P. E.; Cuadrado, T. R. *J. Appl. Polym. Sci.* **1998**, 69, 1367.
38. Kindt-Larsen, T.; Smith, D. B.; Jensen, S., Jr. *J. Appl. Biomater.* **1995**, 6, 75.